A CMOS Visible Silicon Imager hybridized to a Rockwell 2RG multiplexer as a new detector for ground based astronomy

Reinhold J. Dorn*, Siegfried Eschbaumer, Gert Finger, Leander Mehrgan, Manfred Meyer, and Joerg Stegmeier
European Southern Observatory, Karl Schwarzschildstr.2, D-85748 Garching, Germany

ABSTRACT

For the past 25 years Charge Coupled Devices (CCDs) have been used as the preferred detector for ground based astronomy to detect visible photons. As an alternative to CCDs, silicon-based hybrid CMOS focal plane array technology is evolving rapidly. Visible hybrid detectors have a close synergy with IR detectors and are operated in a similar way. This paper presents recent test results for a Rockwell 2K x 2K silicon PIN diode array hybridized to a Hawaii-2RG multiplexer, the Hybrid Visible Silicon Imager (HyViSI). Since the capacitance of the integrating node of Si-PIN diodes is at least a factor of two smaller than the capacitance of the Hawaii-2RG IR detector pixel, lower noise was expected. However, those detectors suffer from interpixel capacitance which introduces an error to the value of the conversion factor measured with the photon transfer method. Therefore QE values have been overestimated by almost a factor of two in the past. Detailed test results on QE, noise, dark current, and other basic performance values as well as a discussion how to interpret the measured values will be presented. Two alternative methods, direct measurement of the nodal capacity and the use of Iron-55 X-rays to determine the actual nodal capacitance and hence the conversion factor will be briefly presented. PSF performance of this detector was analyzed in detail with an optical spot and single pixel reset measurement.

Keywords: Conversion gain, interpixel capacitance, CMOS hybrid, quantum efficiency, Hawaii-2RG, Si-PIN, HyViSI

1. INTRODUCTION

As an alternative to Charge Coupled devices, silicon-based hybrid CMOS focal plane array technology was introduced recently. The detector we have tested is a Rockwell 2K x 2K silicon PIN diode array hybridized to a Hawaii-2RG multiplexer, the Hybrid Visible Silicon Imager (HyViSI). The detector is an optical sensor, analogous to near-infrared (NIR) array detectors. The separation of photon collection from readout facilitates separate optimization of the CMOS Hawaii2RG readout multiplexer (MUX) and the Silicon PIN detector array. The main difference to IR detectors is that for silicon pin the full bulk of the detector is in depletion whereas IR detectors are per pixel depleted detectors. Note that a hybrid differs substantially from a monolithic CMOS imager. In a CMOS imager, both readout and photon detection take place in the same piece of silicon. As nearly the full bulk of the detector is in depletion, silicon PIN detectors have good QE at both red and blue wavelengths. Silicon PIN detectors are operated at very high bias (~10 to 20 Volts) compared to near-IR detectors. Silicon PIN detectors have a fill factor ~100% and offer some advantages compared to CCDs needed for both ground-based and space applications. These advantages include extensive on-chip readout capability with the Hawaii 2RG multiplexer, flexible imaging readout and the ability to provide low noise at high frame rates. For infrared imaging applications that involve UV-through visible channels, the readout electronics commonality facilitates a great simplification to system designs.

*rdorn@eso.org; phone +49-89-32006547; fax +49-89-3202362; www.eso.org/~rdorn

2. CONVERSION GAIN AND NODAL CAPACITANCE

2.1 Photon transfer curve

Measurement of detector parameters such as noise, system gain, full well capacity, quantum efficiency, dark current, sensitivity and linearity are usually covered using the photon transfer curve. The photon transfer curve plots readnoise as a function of the signal for an area of *n* by *n* pixels in a frame. To obtain the x-axis of the curve one computes the mean, dark subtracted signal S. That is

$$S = \frac{\sum_{i=0}^{i=N_p} S_i - S_{dark}}{Np} \tag{1}$$

where S_i is the signal value of the *i*th pixel and N_p is the number of pixels in the *n* by *n* pixel area. S_{dark} is the signal of a dark frame taken from the same data set. To obtain the y-axis of the curve, the variance σ^2 is computed. The variance is the square of the standard deviation of a single observation from the mean of the pixels [Janesick 2001].

$$\sigma^2 = \frac{\sum_{i=1}^{i=N_p} (S_i - S)^2}{Np} \tag{2}$$

This photon transfer curve is a fundamental technique to measure the performance of a detector and to determine the conversion factor (C_0/e) measured in units of electrons per Volt or electrons /ADU. The nodal capacitance C_0 is the capacitance of the integrating node. It is composed of the voltage dependent diode capacitance of the detector pixel and the fixed gate capacitance of the unit cell source follower gate. If the photon energy is small compared to KT with K being the Boltzmann constant and T the blackbody temperature of the radiation source, the variance of the integrated number of photons is equal to the mean number of photons. For this case, the nodal capacitance C_0 can be calculated from the slope of the plot of noise squared signal versus mean signal. However, this method only works if the signals of neighboring pixels are uncorrelated. Current HyViSI detectors suffer from interpixel coupling which attenuates poisson noise and introduces an error of up to 50 % for the conversion factor measured with the signal versus noise method. We measured a conversion gain with our setup of 3.55 electrons/ADU or 178 electrons/mV which led to wrong values by determining the QE of the detector by almost 100%.

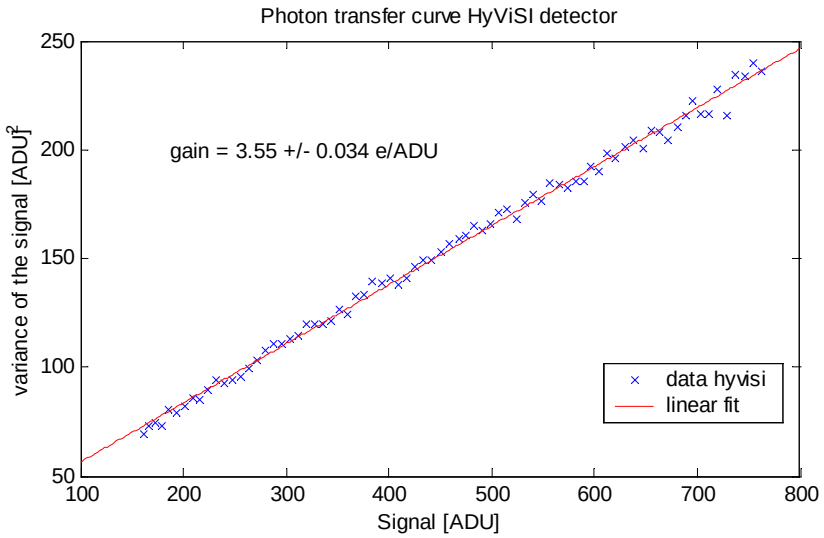

Figure 1 HyViSI conversion factor measured with photon transfer curve in the shot noise limited regime (gain = 178 e/mV).

Hence we tried to measure the conversion factor for the HyViSI with different methods. The first method was to determine the conversion factor with an FE-55 X-ray source.

2.2 FE-55 measurements

FE-55 is a radioactive source that emits X-rays at three energy levels. The emission is caused by the inner electron of the FE-55 isotope being captured by the nucleus, transforming it into Manganese. The first emissions is at 5.9 keV (Mn K_α line), the second but weaker peak at 6.5 keV (Mn K_β) and the third at 4.12 keV (K_α escape line). When these X-rays are absorbed by silicon they produce large photoelectron events. Each K_α event generates 1620 electrons, K_β 1778 electrons and the K_α escape peak 1133 electrons. Occasionally, the absorbed X-ray photon is re-emitted (fluoresced) by the silicon of the detector and is reabsorbed later where it produces a photo-electron event of 487 e, called the silicon line. All of these X-rays are easily stopped with glass or metal. To perform the test with the HyViSI detector a plexiglas window with a thickness of 2 mm was used not to attenuate the X-rays too much to allow enough events on the detector. An FE- 55 source with 1 MBq was used and installed on a special window (see Figure 2).

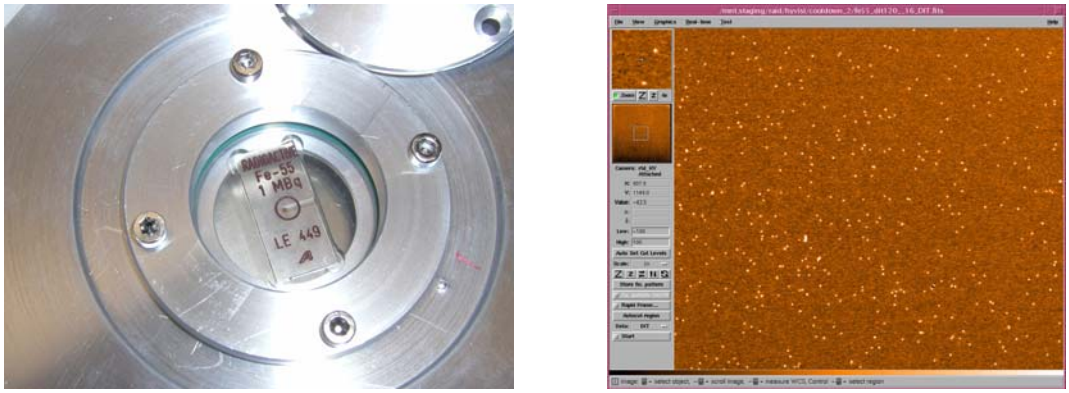

Figure 2 Left picture: FE-55 X-ray source installed on the window in front of the HyViSI detector. Right picture: FE-55 X-ray events on the detector (120s integration time, double correlated readout).

Figure 2 right shows an image of 120s integration time with the X-ray events visible. The readout mode was double correlated. The events have been analyzed with a photometric routine and a histogram has been plotted (see Figure 3).

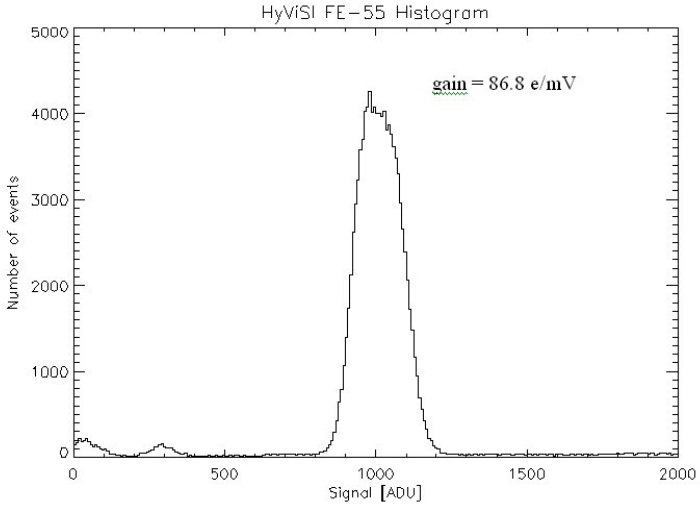

Figure 3 HyViSI FE-55 histogram leading to a conversion factor of 1.65 electrons/ADU or 86.8 e/mV which is a factor 2 smaller than the value measured with the Photon transfer curve.

From the histogram a conversion factor of ~1.65 electrons/ADU was determined. This is a factor of two lower than the conversion factor measured with the photon transfer curve. To verify in more detail this discrepancy a third technique was used to measure the conversion factor independently.

2.3 Capacitance comparison

In order to obtain the nodal capacitance C_0 by a direct measurement which does not rely on statistical methods, a simple but very powerful technique has been developed. It is based on comparing the voltage change of a large calibrated external capacitor to that of the unknown nodal capacitance C_0 which is many orders of magnitudes smaller. This method is described in detail by Finger et al. in 2005. For the HyViSI detector a nodal capacitance 13.9 fF was measured. The discrepancy of nodal capacitances C_0 determined by the capacitance comparison and the shot noise method is substantial and about a factor of two for the HyViSI detector. Thus, plausible quantum efficiencies cannot be achieved using the conversion gain derived from the shot noise method with the usual "noise squared versus signal" technique. The capacitance comparison method confirms the values measured with the FE-55 measurements and leads to the conclusion that the shot noise method is wrong for this device. The following equations explain how the conversion factor and nodal capacitance are related. The following picture shows the schematics of the cryogenic preamp used for one channel of the HyViSI before the signal gets digitized.

Electronic gain of the preamp is:

$$g = 1 + \frac{2 \cdot R_a}{R_m} = 4 \qquad (3)$$

and the conversion factor is:

$$c = \frac{s \cdot C_0}{q \cdot g} \qquad (4)$$

where c is the conversion factor in electrons/ADU, s is ADC sensitivity $5V/2^{16} = 76.3 \times 10^{-6}$ Volt/ADU, g is electronic gain of the preamp (4), G is conversion gain in electrons/Volt and q is the electron charge 1.60218×10^{-19} C or As. The conversion factor in e/ADU is 1.65 electrons/ADU.

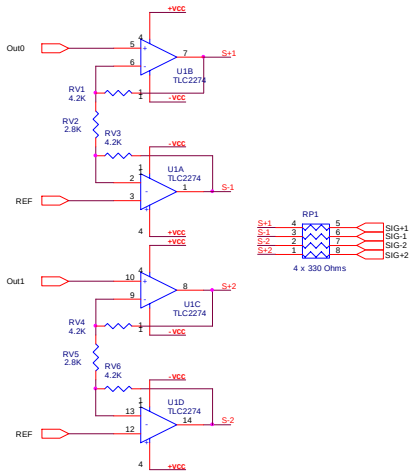

Figure 4 Preamplifier and gain for one video channel.

2.4 Discussion of Results

The shot noise method leads to different and wrong values because the detector pixels of the HyViSI suffer from capacitive coupling to its neighboring pixels [Moore 2003]. This interpixel capacitance causes Poisson noise to appear smaller and hence the conversion factor to be larger. The responsive quantum efficiency is overestimated as the device appears to sense more photons than actually arrive on the pixel. This will be explained in more detail later. Note that capacitive coupling is deterministic and should not be mixed up with the effect of charge diffusion. The conversion gain measured for HyViSI using Iron-55 x-rays and the capacitance measurement method both determine the total conversion gain and need to be applied for QE measurements. For the QE the entire array is uniformly illuminated and thus the amount of "gain" lost from a node with charge to neighboring pixels is received back from the neighboring pixels since all are at the same light level. For the readout noise this conversion factor can only be used partly. Since we are measuring and calculating the readout noise of a single node, the total conversion factor in e/ADU will be too low. However the conversion gain used for all measurements and results is the one measured with FE-55 in this paper. It underestimates noise by a certain factor. The author thinks that it is important to state the method the conversion gain has been measured for all parameters.

3. QUANTUM EFFICIENCY

3.1 Setup and method

With the exact measurement of the conversion gain it was now possible to measure quantum efficiency for the hybrid detector. Figure 5 shows a schematic of the used setup and a picture of the cryostat mounted to the testbench.

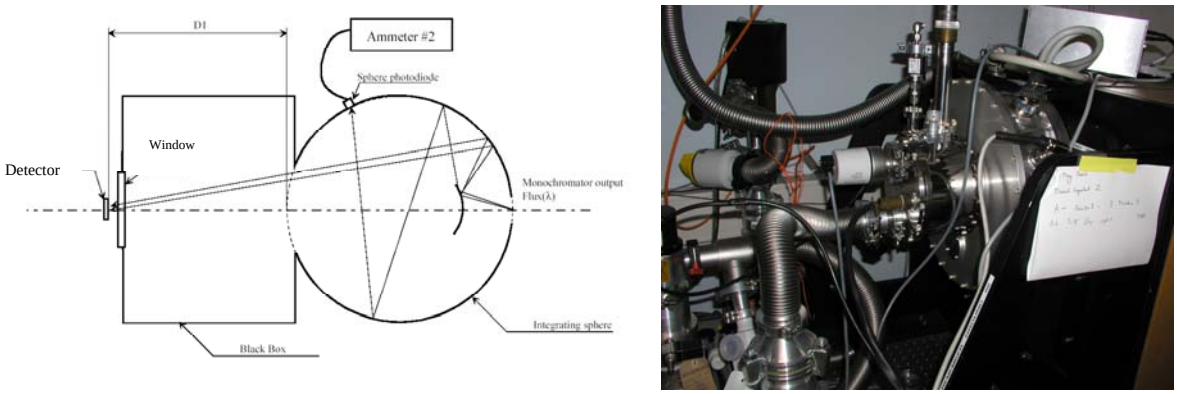

Figure 5 Left: Setup for the QE measurement. Right: Picture of the cryostat mounted to the testbench.

The QE of the detector was measured by comparing the sensitivity of the detector and an absolute calibrated reference diode.

$$QE(\lambda) = \frac{A_{diode} \cdot S_{\det} \cdot QE_{diode}}{P_s \cdot \frac{I_{diode}}{q \cdot r_{diodes}}} \tag{5}$$

$$S_{\det} = \frac{S_{adu} \cdot c}{t_{\exp}} \tag{6}$$

were QE(λ) is the quantum efficiency of the detector, A_{diode} is the active area of the diode in cm^2 ($1cm^2$), S_{det} is the signal of the detector pixel or window (mean) electrons/pixel/s, c is the conversion factor in (e/ADU), t_{exp} is the exposure time in s, QE_{diode} is the QE of the reference diode, P_s is the active area of a pixel (cm^2), I_{diode} is the signal of the reference diode (A), q is the electron charge 1.6021 x 10^{-19} C or As, S_{adu} is the signal in ADU and $r_{diodes=}I_{diodesphere}/I_{dioderef}$.

3.2 QE Results

Quantum efficiency has been measured at temperatures ranging from 120 to 200 Kelvin in steps of 20 Kelvin to reveal its temperature dependence. The device shows a temperature dependent QE which is due to the photon absorption length. As the temperature gets lower, the absorption length increases. This is due to the bigger band gap a lower temperature. In the near IR this is more important as Phonons help to energize free electrons in the conduction band. However the device shows excellent broad band QE and outperforms many CCDs above 500 nm and also shows a higher overall QE compared to the CCDs. The QE results fit very well with a modeled curve by Rockwell. For comparison Figure 7 shows QE curves for the HyViSI detector, an astro curve provided by e2v for a broad band deep depletion device, a 2 layer AR coating of the deep depletion e2v CCD and the QE of the CCD currently installed in the Giraffe spectrograph at the VLT. Additionally a measured QE curve of an IR Hawaii2RG HgCdTe detector is shown.

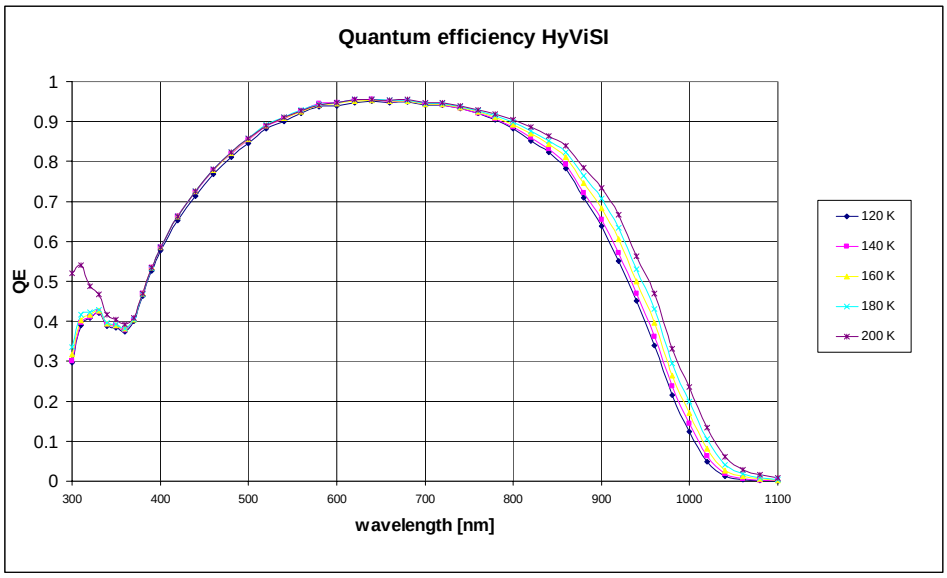

Figure 6 HyViSI QE at various temperatures.

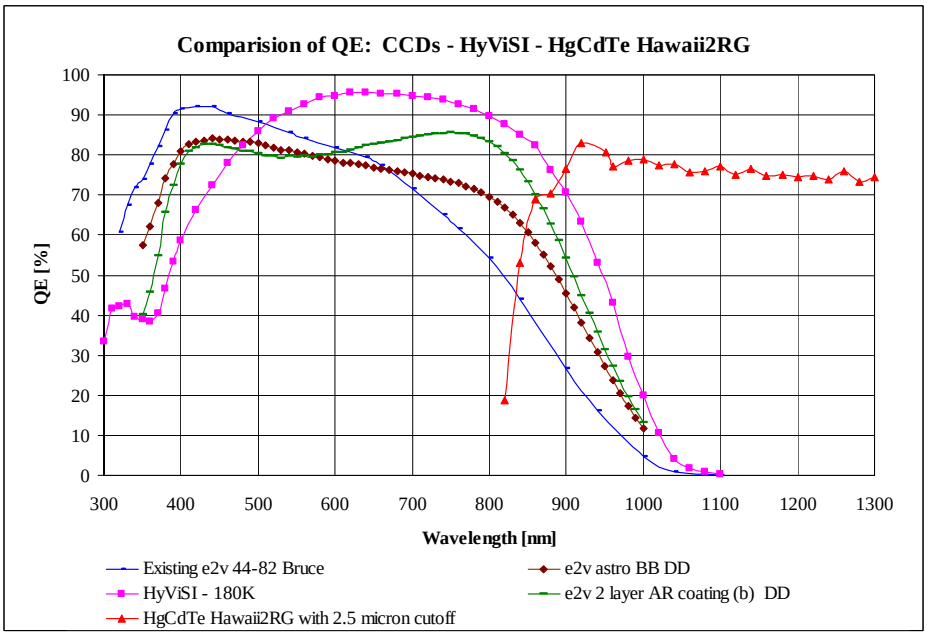

Figure 7 Comparison of candidate CCDs for an upgrade of the Giraffe spectrograph at the Very Large Telescope and QE for a Hawaii2RG HgCdTe detector with 2.5 microns cutoff wavelength.

4. DARK CURRENT

Dark current has been measured for temperatures down to 110 Kelvin and bottoms out at 3 x 10^{-3} electrons/sec below 140 Kelvin for this eng. device (Figure 8). Darkcurrent values might be lower with science grade devices but for the engineering grade the darkcurrent is around a factor 10 higher than that of scientific CCDs which is around one electron per hour.

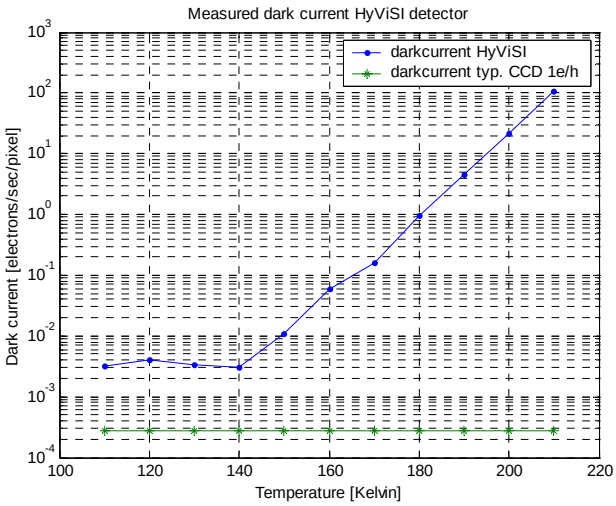

Figure 8 Darkcurrent as a function of temperature.

5. READOUT NOISE

Readnoise was measured as a function of Fowler pairs at different temperatures. The device shows a strong temperature dependence which can not be explained by Johnson noise but follows 1/sqrt(n) for Fowler sampling. The reason for this temperature dependence is not yet known but has been addressed to the manufacturer. Noise is 6 electrons for a single DC read (readtime ~1 sec) and as low as 1.8 electrons for 30 Fowler pairs (readtime ~25 sec) at 120 Kelvin with a conversion gain measured with the FE-55 method. Figure 9 plots the number of fowler pairs versus readout time. Note that the readnoise does not improve with more samples.

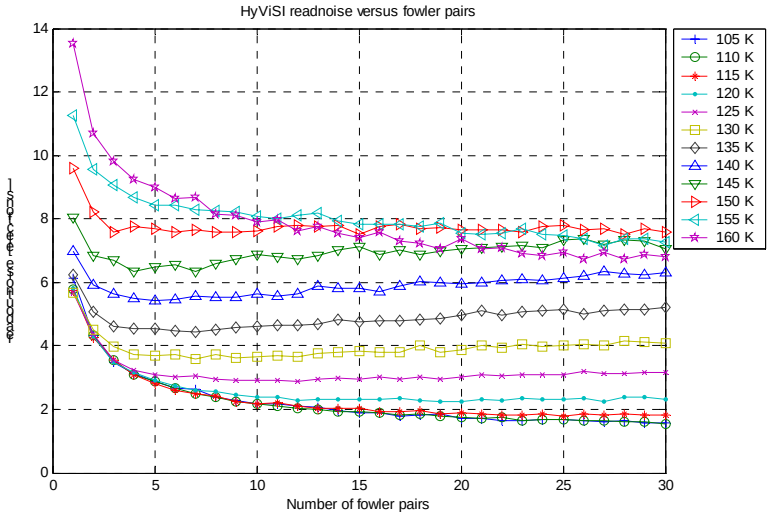

Figure 9 Readout noise at different temperatures (linear plot).

6. LINEARITY

Hybrid detectors are inherently non-linear compared to CCDs. As photons discharge the diode capacitor, the bias voltage across the junction gets smaller and hence the nodal capacitance increases. This also introduces an error in the

measurement of the conversion factor. Linearity has been measured for signal levels ranging from 850 to 90000 electrons and the detector shows a residual non linearity of ~5% (p-v) for a bias voltage of Dsub =10Volts. The error fraction is (mean signal value divided by the fitvalue)-1.

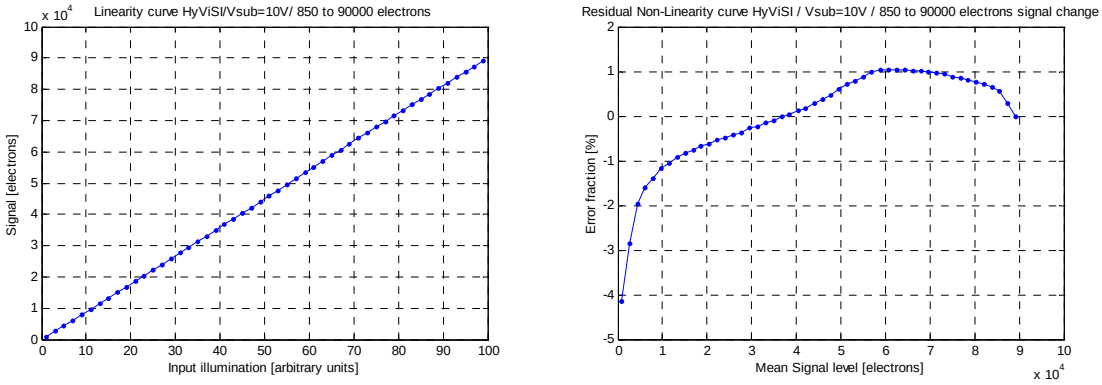

Figure 10 Linearity curve for signal levels ranging from 850 to 90000 electrons at a bias voltage of 10 Volts.

7. INTERPIXEL COUPLING

The pixels for this detector couple capacitively to their neighboring pixels. We call this interpixel capacitance. The coupling capacitors reduce the photon shot noise because the voltage response of a photon-generated electron is not contained within a single pixel, but spread over all neighboring pixels. This nominal reduction of noise is accompanied by reduced image contrast and degraded detector PSF. The HyViSI is a Si-PIN diode array hybridized to the Hawaii-2RG multiplexer but has much larger interpixel coupling capacitances (coupling around 42%) compared to the HgCdTe infrared array (coupling around 9%) [Finger et al. 2005]. The main contribution to interpixel capacitance is not located in the multiplexer or between the indium bumps but in the Si-PIN bulk itself. The main difference between the SI and IR arrays is that an SI Hybrid is a fully depleted bulk detector whereas the IR array is a per pixel depleted detector (see Figure 11). IR detectors have a separate depletion region close to the pixel implant. For the SI array there is a metal grid which reduces the coupling between the In-bumps and therefore most of the coupling is within the bulk of the detector. For the infrared array there is no electric field in the bulk so that coupling is not possible there. Here the coupling occurs between the MUX and the detector material [Moore et. al. 2003]. Capacitive coupling between detector pixels is a deterministic process which conserves photometry and can be accounted for, if properly calibrated. In the photon noise limited regime both the signal and the noise are attenuated by the same factor. To measure the quantity of capacitive coupling in the HyViSI a single pixel reset and a spot measurement were done and are described in the following sections.

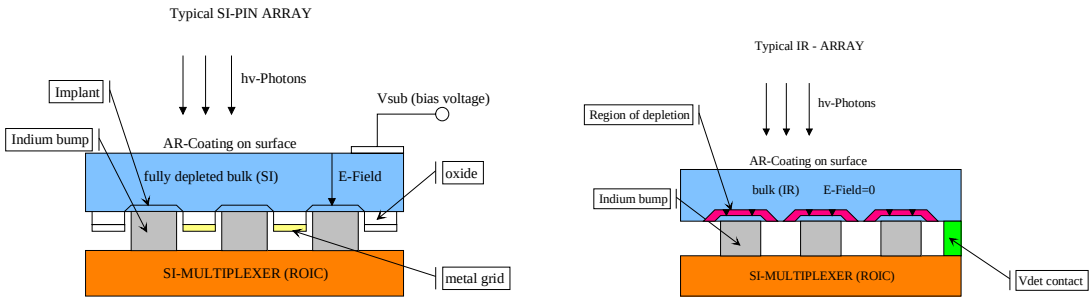

Figure 11 Left: Typical SI Hybrid (most of the cap. coupling is within the bulk) Right: Typical IR array (most of cap. coupling is between the mux and the bulk).

7.1 Single pixel reset test

To quantify the capacitive coupling between pixels for the HyViSI detector the guide mode feature of the Hawaii2RG multiplexer was used to reset a single pixel and hence to measure the resulting spread of charge around the center pixel. Here the array is uniformly illuminated with high flux and by resetting a single pixel with the guide mode feature of the 2RG mux its value is set to zero [Finger et al. 2005]. Figure 12 shows a single pixel reset image of the HyViSI detector and its surface plot, the normalized response of neighboring pixels with single pixel reset. Note that the maximum value of Z is 0.3. Central pixel has intensity 1.

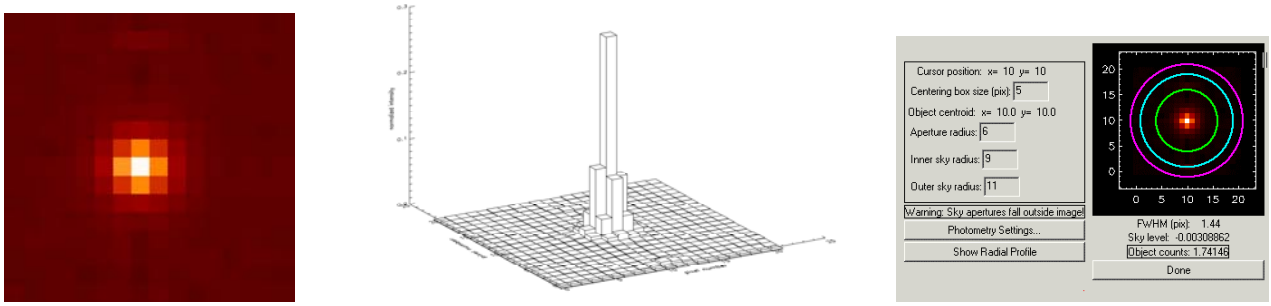

Figure 12 Single pixel reset image of the HyViSI detector and surface plot of the pixel at 10 Volts Vsub. Photometric analysis at 10 Volts bias voltage on the right.

With a photometric analysis of the image (Vsub = 10 V) the total normalized signal is 1.74 as seen above. That means that 42 % of the total energy is spread to neighboring pixels. The coupling to the next neighbors is 8 to 10 %. For Vsub at 5 Volts around 45% of the total energy is spread to neighboring pixels. For voltages higher than 10 Volts no improvement of PSF is seen.

7.2 Optical spot measurement

To confirm the measurements done with the single pixel reset method, an optical spot having a diameter of < 5 microns on the detector was used to illuminate a single pixel and measure the crosstalk to neighboring pixels. Before projecting the spot on the detector, its diameter was measured optically with a microscope setup. After that the optics was mounted on a xyz stage and the spot was focused onto the detector.

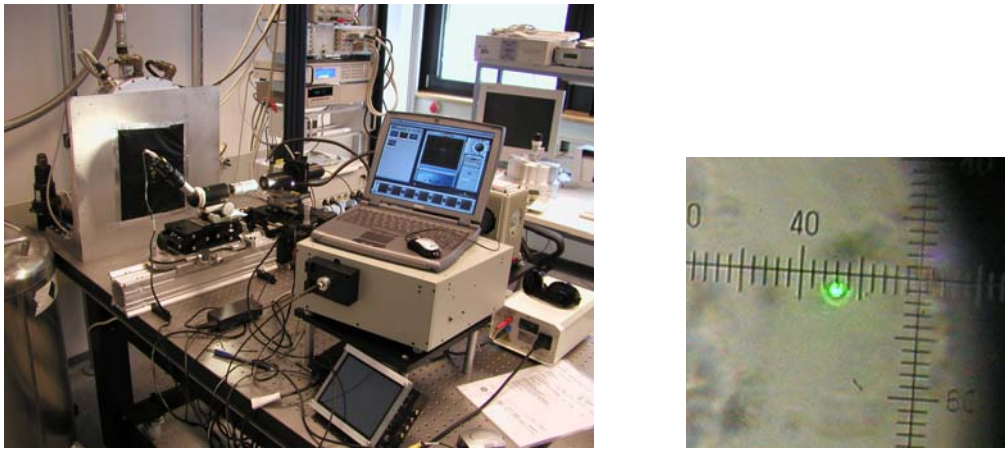

Figure 13 Setup to measure optically the quality and size of the spot to measure interpixel capacitance and resulting spot of 4 to 5 microns in diameter. The distance between two scale lines is 2.6 microns.

Similar to the method before a photometric analysis of the spot was done (Vsub = 10V) and the total normalized signal is 1.77 as seen in Figure 14. Those optical measurements confirm that most of the crosstalk is due to the interpixel capacitance and charge diffusion plays a minor role. 43.5 % of the total energy is spread to neighboring pixels and the coupling to the next neighbors is ~8-10 %. This is about the same result as for the single pixel reset measurement. To measure the sensitivity profile of a single pixel a more stable mechanical setup is required. We plan to purchase a new motorized xyz-stage to perform a spot scan measurement.

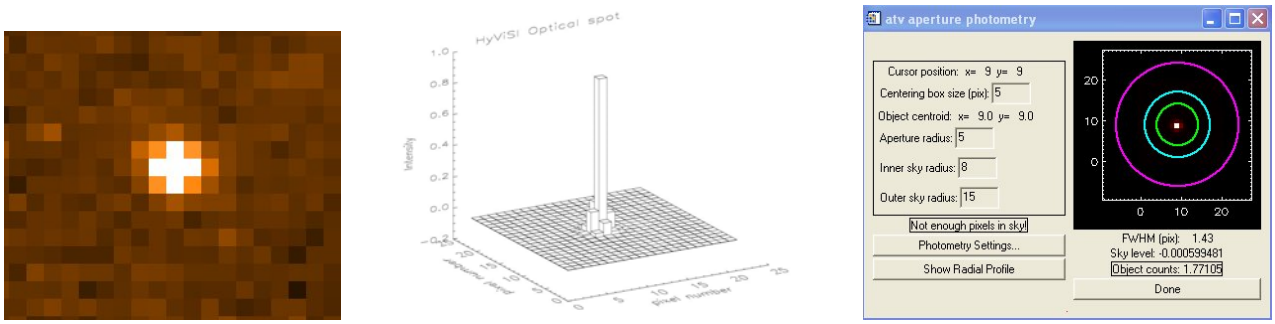

Figure 14 Optical spot (5 microns) projected onto the detector and surface plot of the optical spot. Photometry of the optical spot (43.5 % of the total energy is spread over neighboring pixels).

8. COSMETIC QUALITY

The cosmetic quality of the tested eng. grade device depends very much on the operating temperature. Below is a summary of pictures taken at different temperatures. The images are taken with an exposure time of 20 seconds, 24 Fowler pairs, a somewhat typical mode for imaging. We observe 3 main features on the detector:

- defective pixels
- glow centers in inner part of the detector area
- glow centers at edges

At low temperatures and low dark current up to 160 Kelvin one can observe some glow areas on the right and upper edge of the detector but glow spots in the middle of the area seem to be frozen out. For temperatures above 160 Kelvin glow centers all over the device are more dominant. Note that this is an eng. grade device and the glow spots might be less on a science grade arrays.

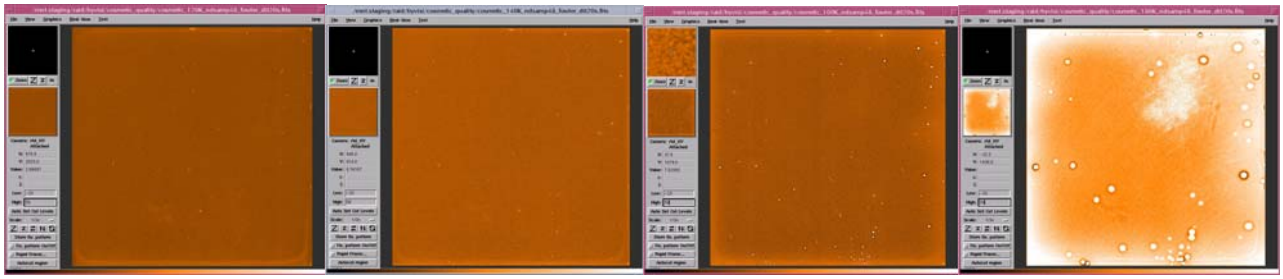

Figure 15 Dark images showing the cosmetic quality of the detector. Pictures taken at 120 Kelvin, 140 Kelvin, 160 Kelvin and 180 Kelvin operating temperatures from left to right- 24 fowler pairs and 20 sec exposure time.

9. RESIDUAL IMAGE/PERSISTANCE

Latent charge, or “persistence,” is the remaining signal apparent in a series of dark exposures, after the array has been exposed to a bright radiation source. Any process which, after some delay, releases charge into the conduction band can contribute to latent charge. Latent charge is a function of photon flux during a previous exposure and the time elapsed

since the previous exposure as shown in Figure 16 and 17. The measurements were done with monochromatic light projecting the output slit of the monochromator onto the detectors.

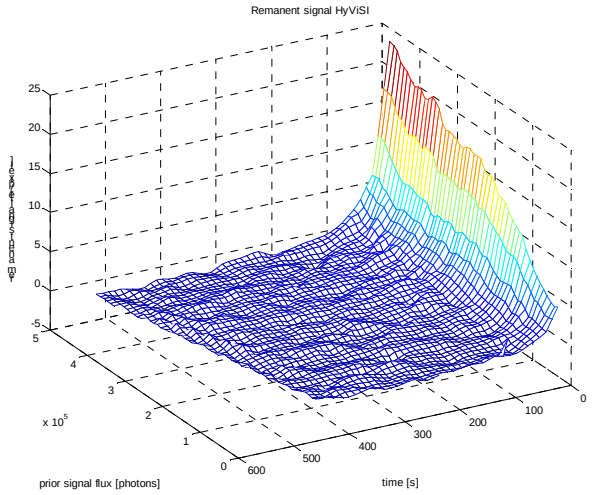

Figure 16 Decay of residual image as a function of time and prior photon flux.

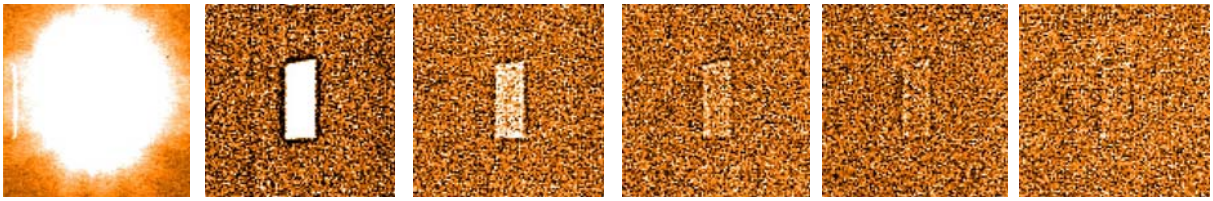

Figure 17 Decay of residual image intensity as a function of time and prior signal flux. The right image shows an overexposed and highly saturated image with ~330K electrons and then the shutter was closed and several readouts with 25s integration time each were taken. The second image was taken after 25s, the next after 75s, then 150s, 225s and finally after 475 seconds.

10. FINGING AT RED WAVELENGTH AND FLATFIELDS

The following pictures show flat field images of the detector at different wavelength. Above 900 nm the detector show fringing patterns depending on the thickness of the detector material.

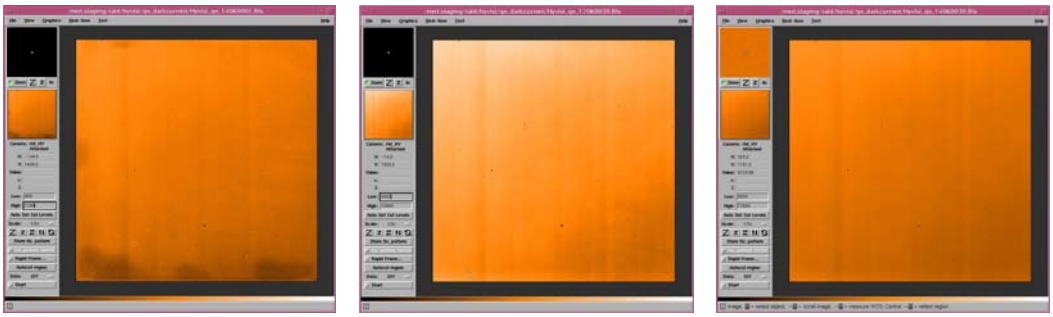

Figure 18 Flatfield at 350 nm, 600 nm and 800 nm at 140 Kelvin.

Figure 19 show an image at 900 nm with a maximum fringing in the left upper corner of 4 % of the signal level. At 960 nm the fringing is around 6 % and at 1000 nm the maximum fringing is at the 8% signal level.

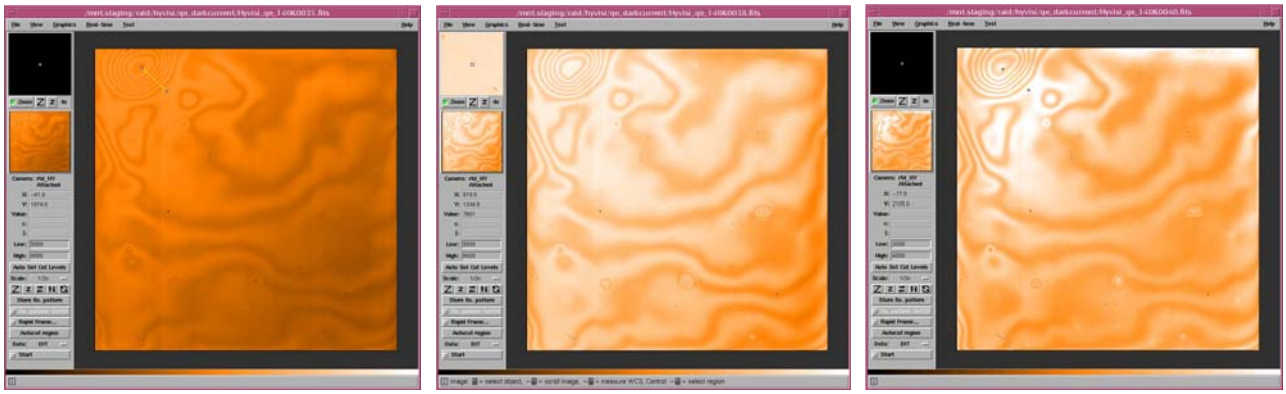

Figure 19 Flatfields at 900 nm, 960 nm and 1000 nm at 140 Kelvin.

11. CONCLUSION

The tested detector is a Hybrid Visible Silicon Imager (HyViSI) from Rockwell Scientific. It is a complementary metal oxide semiconductor (CMOS) alternative to charge coupled devices (CCDs) for photons at optical wavelengths. The tested device has high broad band quantum efficiency which peaks at 95 % at 650 nm and outperforms most CCDs with the same material thickness. QE has been measured from 120 to 200 Kelvin and shows a typical temperature dependence which is due to photon absorption length. The device suffers from interpixel capacitance which introduces an error in the determination of the nodal capacitance or conversion factor with the standard photon transfer method and degrades PSF of a point source. The interpixel coupling has been analyzed in detail with a single pixel reset measurement and around 43 % of the total energy of a pixel is seen in neighboring pixels. Coupling to closest neighbor pixels is around 8 to 10 %. This effect is a deterministic coupling mechanism and not diffusion. Optical spot measurements confirm the single pixel reset measurements. Darkcurrent and readnoise have been measured as a function of temperature from 120 to 200 Kelvin. Lowest values for the darkcurrent have been measured at < 140 Kelvin. The obtained values are 3 x 10^{-3} electrons/second or around 11 electrons per hour. Noise depends very much on operating temperature but follows 1/sqrt(n) for Fowler sampling. The reason for this temperature dependence is not yet known but has been addressed to the manufacturer. Noise is 6 electrons for a single DC read (readtime ~1 sec) and as low as 1.8 electrons for 30 Fowler pairs (readtime ~25 sec) at 120 Kelvin with a conversion gain measured with the FE-55 method. The cosmetic quality can be significantly improved by proper cooling of the detector below 120 to 130 Kelvin. For higher temperatures the device shows various glow centers around defective pixels. At wavelengths around 980 nm the device shows some weak fringing. Persistence is negligible for signals up to full well but can be seen on highly over-exposed images. The tested detector has compatible performance to scientific CCDs and also offers some advantages. These advantages include higher QE, extensive on-chip readout capability with the Hawaii 2RG multiplexer, flexible imaging readout and the ability to provide low noise at high frame rates. No shutter is required and less power needed. The common readout electronics with IR arrays facilitates a great simplification to system design. Soon this device will be able to be read out with an ASIC in 32 channel mode.

REFERENCES

1. Gert Finger, James W. Beletic, Reinhold J. Dorn, Manfred Meyer, Leander Mehrgan, Alan F. Moorwood and Joerg Stegmeier, Conversion gain and interpixel capacitance of CMOS hybrid focal plane arrays, Workshop on Scientific Detectors for Astronomy, Springer-Verlag, (2005).
2. J. R. Janesick, Scientific Charge-Coupled Devices, SPIE Press, p. 134, (2001).
3. Gert Finger, James Garnett, Naidu Bezawada, Reinhold J. Dorn, Leander Mehrgan, Manfred Meyer, Alan Moorwood, Joerg Stegmeier and Guy Woodhouse, Performance evaluation and calibration issus of large format hybrid active pixel sensors used for ground and space based astronomy, Nuclear Inst. and Methods in Physics Research A, 2005
4. A. Moore et al, QE Overestimation and Deterministic Crosstalk Resulting from Inter-pixel Capacitance, Opt. Eng. (2003).